Jumping robots: a biomimetic solution to locomotion across rough terrain

2007 Bioinspir. Biomim. 2 S65

(http://iopscience.iop.org/1748-3190/2/3/S01)

Bioinsp. Biomim. **2** (2007) S65–S82 doi:10.1088/1748-3182/2/3/S01

Jumping robots: a biomimetic solution to locomotion across rough terrain

Rhodri Armour, Keith Paskins, Adrian Bowyer, Julian Vincent and William Megill

Centre for Biomimetic and Natural Technologies, Department of Mechanical Engineering, University of Bath, Claverton Down, Bath BA2 7AY, UK

E-mail: R.H.Armour@bath.ac.uk, K.E.Paskins@bath.ac.uk, A.Bowyer@bath.ac.uk, J.F.V.Vincent@bath.ac.uk and W.M.Megill@bath.ac.uk

Received 14 December 2006
Accepted for publication 18 May 2007
Published 22 June 2007
Online at stacks.iop.org/BB/2/S65

Abstract
This paper introduces jumping robots as a means to traverse rough terrain; such terrain can pose problems for traditional wheeled, tracked and legged designs. The diversity of jumping mechanisms found in nature is explored to support the theory that jumping is a desirable ability for a robot locomotion system to incorporate, and then the size-related constraints are determined from first principles. A series of existing jumping robots are presented and their performance summarized. The authors present two new biologically inspired jumping robots, Jollbot and Glumper, both of which incorporate additional locomotion techniques of rolling and gliding respectively. Jollbot consists of metal hoop springs forming a 300 mm diameter sphere, and when jumping it raises its centre of gravity by 0.22 m and clears a height of 0.18 m. Glumper is of octahedral shape, with four 'legs' that each comprise two 500 mm lengths of CFRP tube articulating around torsion spring 'knees'. It is able to raise its centre of gravity by 1.60 m and clears a height of 1.17 m. The jumping performance of the jumping robot designs presented is discussed and compared against some specialized jumping animals. Specific power output is thought to be the performance-limiting factor for a jumping robot, which requires the maximization of the amount of energy that can be stored together with a minimization of mass. It is demonstrated that this can be achieved through optimization and careful materials selection.

M This article features online multimedia enhancements

1. Introduction

The aim of the research reported in this paper is to produce a small, autonomous and inexpensive jumping robot for traversing irregular terrain. It will use a locally-available energy resource. Given the breadth of successful jumping organisms present in nature, biomimetics will deliberately be used to aid the design and development.

The majority of robot locomotion utilizes wheels, which are very efficient at covering smooth terrain, but these vehicles are unable to pass obstacles of greater than half their wheel diameter. One exception is Shrimp, a space rover designed for improved mobility which has its wheels mounted on high, articulating bogeys, enabling it to climb obstacles of up to twice its wheel diameter (Estier *et al* 2000). Wheeled robots tend to have good manoeuvrability and could skirt around some obstacles, but others, such as a flight of stairs, walls or perimeter fences, would still halt progress completely.

Walking robots are better able to cope with rough terrain, but generally rely on more complex control systems. The multiple degrees of freedom required for each leg demand several actuators to control them, meaning that the power and computational requirements are likely to be large. There are some novel 'legged' robots with very few actuators such as RHex (Altendorfer *et al* 2001) and Whegs™ (Quinn *et al* 2002), which combines the simplicity of wheels with the adaptability of legs. However, although legged vehicles have a surprising ability to clamber over rough terrain, they are unlikely to get past obstacles of higher than double their leg length.

Tracked vehicles are often chosen for traversing rough terrain but there are still limitations on the maximum obstacle height that can be overcome. This height is dependent on various factors including the dimensions of a tracked unit, the positioning of its centre of gravity and the friction between the track and the terrain. Tracked robots are typically dimensioned specifically for the terrain requirement and therefore it is difficult to determine a generic maximum obstacle height. Lui (2005) presents a useful analysis of the stair-climbing ability of a simple tracked robot which results in a maximum obstacle height but this is representative of a specific case only. Obstacles that are taller than half the length of a tracked robot are likely to be impassable unless the centre of gravity is far from the geometric centre of the device.

In summary, traditional ground robot locomotion techniques seem to be limited to traversing obstacles of a similar order of magnitude as their size. Jumping robots may be able to traverse obstacles an order of magnitude larger than their own size.

As the size of a moving object decreases, it becomes more likely to meet an obstacle of similar or larger size to itself, and therefore it will encounter rough terrain more often. This is called the 'size-grain hypothesis' (Kaspari and Weiser 1999) which is defined as an 'increase in environmental rugosity with decreasing body size'. So a small robot, whether it walks, rolls or jumps will need the ability to cover rough terrain more frequently than a larger robot.

The most effective way of travelling over rough terrain would be to fly over it. Micro-air vehicles are not hindered by obstacles on the ground, but are energetically expensive, resulting in limited power-source life or power requirements that cannot be met continuously from the surroundings, and are hence unsuitable for some applications. The periodic nature of jumping allows time for recharging energy from the surroundings, making it a more sensible approach to designing a fully-autonomous rough-terrain robot.

Looking at nature, we find that many animals employ jumping as a tactic for traversing obstacles. Some jump to escape predators or capture food, while for others, such as kangaroos, it is the favoured method of locomotion. There are two distinct jumping patterns that can be observed. Locusts, for example, travel using single jumps followed by a rest period to recharge and re-orientate (Bennet-Clark 1975). This can be categorized as the 'pause and leap' method and is common in insects and other small animals such as frogs. The alternative approach is continuous hopping, where energy is recovered during the landing and used in the following jump, a technique employed by kangaroos in order for them to travel large distances across the bush (Alexander and Vernon 1975). Continuous hopping requires a higher level of sophistication in control, and this, combined with the lack of recoverable kinetic energy due to insects small mass means that all the insect jumpers are in the 'pause and leap' category. They tend to have little or no control in the air, landing ungracefully before getting back to their feet and sometimes launching again.

In order for a biological system to achieve its largest jump, it needs to produce the maximum amount of energy in a single event. In nature, muscles are the most common means of initiating locomotion. These have the ability to either shorten or generate tension and if they do both simultaneously, they can perform mechanical work (Bennet-Clark 1976). (It is also possible to store muscular energy for jumping in spring-like structures; this will be covered below.) Neglecting air resistance and losses due to the slipping of the feet on the ground, all the work done by the animal will be converted directly into kinetic energy:

$$KE = \tfrac{1}{2}mv^2 \tag{1}$$

where m is the mass of the animal, and v is its take-off velocity. The kinematic equations for calculating the maximum height and range of ballistic projectiles ignoring wind resistance are well known.

Peak height, h:

$$h = \frac{(v\sin\theta)^2}{2g}. \tag{2}$$

And maximum range, x:

$$x = v^2\frac{\sin 2\theta}{g} \tag{3}$$

where g is the acceleration due to gravity and θ is the take-off angle. These equations and all subsequent kinematic equations can be found in any elementary physics text book. It is clear from (3) that the maximum horizontal range is achieved when the take-off angle is 45°. Likewise, in order to maximize the height of a jump, the ideal take-off angle is 90°. By combining either equation (2) or (3) with equation (1), we see that both the maximum height h, and the maximum range x, are proportional to the energy, or work done by the muscle, divided by the total mass. Therefore, by assuming that the amount of mechanical work done by a muscle is proportional to its mass (Gabriel 1984), then the jumping performance is dependent on the percentage of the body that is muscle directly involved in the jump. It follows then that if the proportion of the body mass taken up by jumping muscle is consistent across a range of animal sizes, and neglecting other factors such as air resistance, all animals should in theory be able to jump to the same height (Hill 1950). However, Henry Bennet-Clark suggests that larger animals are limited by the maximum amount of mechanical work which their jumping muscles are capable of developing, whereas the performance of smaller animals is limited by high power requirements (Bennet-Clark 1977). What the first half of this statement means is that larger animals would have to dedicate a higher proportion of their total mass to jumping muscles. Looking in more detail at this latter point, the energy required for a jump is usually applied to the ground through extension or rotation of the legs, and the take-off force can only act while these are in contact with the ground. Therefore, the length of the leg also has a direct influence on jumping performance and in order to overcome this many insects and small animals use 'biological catapults'—energy storage mechanisms—as a means of generating higher power from their muscles. The proof that shorter leg length requires higher power actuation is given below.

The equation for an accelerating body is

$$v^2 = u^2 + 2as \tag{4}$$

where u is the initial velocity, a is the acceleration and s is the distance through which it is accelerating, which in biology is typically directly proportional to the leg length. Therefore, from equations (2), (3) and (4), again we can see that the height and range will improve directly with increased leg length.

The power output, P, can be related to either energy or force using the standard equations (5) and (6):

$$P = \frac{\text{energy}}{\text{time}} \tag{5}$$

$$P = Fv = mav. \tag{6}$$

Therefore, for an animal jumping from rest, (4) and (6) can be combined to give

$$P = \frac{mv^3}{2s}. \tag{7}$$

Hence, the smaller the leg length, the higher the specific power requirement to reach a given take-off velocity, and therefore range and height.

By combining (2) and (7), we get the following equation which relates power, mass and acceleration distance to height, h, for a vertical jump (Bennet-Clark 1977). This equation will be used later on to evaluate jumping robot performance:

$$h = \left(\frac{2sP}{m}\right)^{\frac{2}{3}} \times \frac{1}{2g}. \tag{8}$$

Owing to their small size, an insect's leg length is limited and on top of this, insects are more affected by air resistance so power amplification is essential for jumping. As a result, many different specializations have evolved in insects to enable effective jumping, some of which have even developed so far as to hinder simple walking (Bennet-Clark 1977). Grasshoppers and locusts have metathoracic legs that are only used for jumping and that are very much larger than the other pairs of legs that are primarily used for walking and stability. It was shown by Bennett-Clark (1975) that locusts are able to achieve a large jumping impulse by moving these legs at a velocity much higher than is possible by direct muscle action by pre-loading energy into a quick-release mechanism. Energy is stored in spring-like cuticular elements by the extensor leg muscles after a physical catch has been engaged (Heitler 1974). This elastic energy storage is comparable with a catapult, which is pulled back slowly against a high force, and then travels much faster when released. Other examples of such catapult mechanisms include fleas (Bennet-Clark 1975, Bennet-Clark and Lucey 1967, Rothschild *et al* 1975) and froghoppers (Burrows 2003), both of which are very small but can jump more than 100 times their body length. Bi-stable mechanisms inherent in their structure are also used by some insects to store energy for jumping including springtails (Brackenbury and Hunt 1993) and click beetles (Evans 1973).

Power amplification is by no means restricted to the insect jumpers. Even larger animals, such as dogs, which use direct actuation of muscles to jump, can generate more power by storing energy in tensile elastic elements during a counter-movement immediately prior to jumping (Alexander 1974).

Another point to consider is that in order to maximize either distance or height, the energy-to-mass ratio must be as large as possible (equations (1)–(3)). The physical size has no effect on the jump unless air resistance is considered. Increased energy requires stronger structures to react the higher forces, but improving strength generally increases the mass thus negating some of the benefit of higher energy levels. To minimize the requirements on the structure, the force should remain constant, below a threshold, throughout the time of the jump rather than peak. Constant force would imply constant acceleration, and hence velocity and power would rise linearly with time to a maximum at take-off.

Owing to the low density energy availability specified for our jumping robots, the 'pause and leap' strategy will be much more suitable than 'continuous hopping'. This allows a robot as much time as necessary to recharge and re-orientate itself between jumps. In principle, jumping robots should be able to clear obstacles much larger than themselves with simple construction and direction control. This could enable a jumping exploration robot to be smaller and cheaper than the equivalent wheeled or walking robot, which would be particularly desirable for space applications where volume and mass are at such a premium. There is also potential for many simple jumping robots to be employed together, in place of a single conventional robot, allowing a semi-sacrificial team mission strategy to be employed.

2. Existing designs

This section highlights a series of existing pause-and-leap jumping robots, grouped by energy storage medium and the capabilities of each are summarized later in table 4. Most existing jumping robots can operate under earth gravity, but there is an important range of microgravity jumping robots that are not discussed here since their application is specifically for very low gravity environments such as surface exploration of asteroids and other interstellar bodies (Nakamura *et al* 2000, Raibert 1986, Shimoda *et al* 2002, Yoshimitsu *et al* 2003). Other 'jumping' robots not described here include a series of hopping robots which continuously jump (Brown and Zeglin 1998, Okubo *et al* 1996, Paul *et al* 2002, Raibert 1986, Wei *et al* 2000). This is because of different design problems which include active balancing and dynamic stability.

2.1. Coil spring based designs

Researchers at NASA Jet Propulsion Laboratories (JPL) and Caltech have developed a series of jumping robots called 'Hoppers' (Fiorini and Burdick 2003)—one of which is pictured in figure 1(a). Of the coil spring designs mentioned here, these robots jump the highest. Each is based around a six-bar linkage and coil spring leg mechanism and it is this that is the most interesting feature. The force–displacement profile of this leg system results in a nonlinear spring profile that has been produced from a linear coil spring. This gradual increasing release force rises to a peak before it reduces, ensuring that the acceleration of the device rises for as long as possible until take-off. This is in contrast to a typical spring where the force

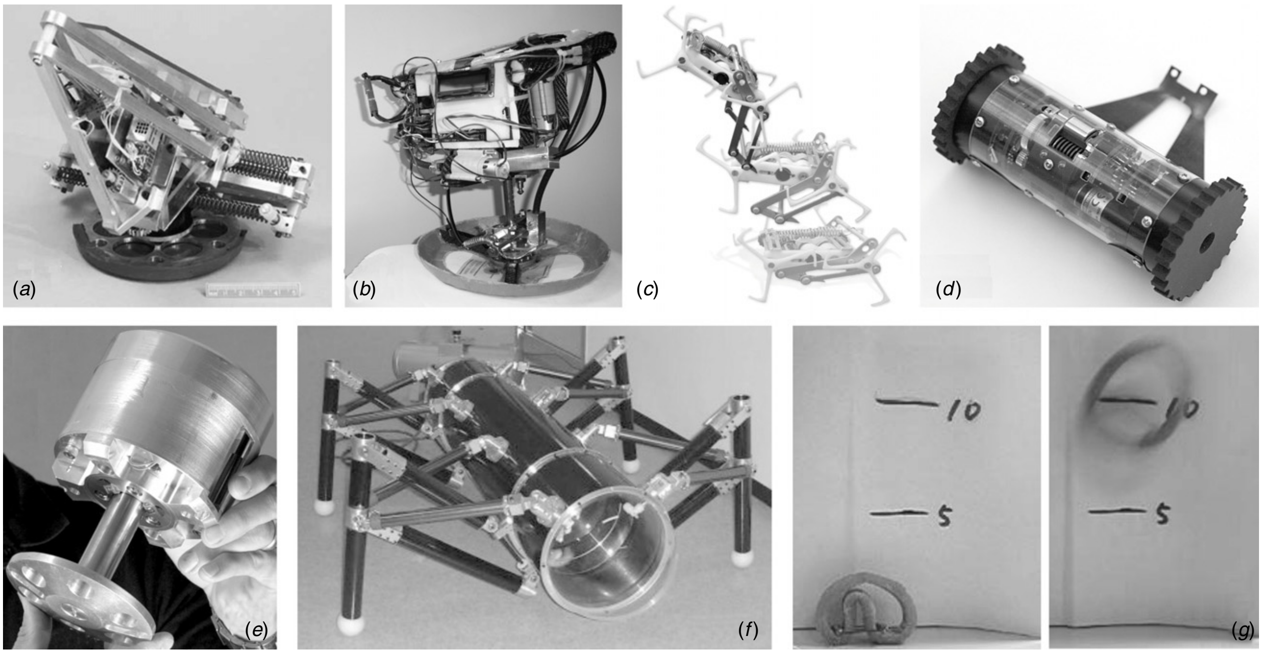

Figure 1. Existing jumping robots: (*a*) JPL Hopper (prototype 2) courtesy NASA/JPL-Caltech, (*b*) Monopod hopper courtesy of James Allison, (*c*) Jumping Mini-Whegs^{TM} courtesy of Case Western Reserve University, (*d*) Scout robot courtesy of University of Minnesota, (*e*) Sandia Hopper courtesy of Sandia Corporation, (*f*) Airhopper courtesy of Tokyo Institute of Technology, (*g*) Deformable Soft Robot courtesy of Ritsumeikan University.

would be highest at the start. This is very important for light weight jumping robots which may undergo premature lift-off (Hale *et al* 2000) where the device jumps before all of the energy is released.

The coil spring based robot that achieved the second greatest leap is the Monopod robot developed by Allison (2002) at the University of Utah—a photograph of which is presented in figure 1(*b*). Unlike the JPL hopper, here the coil spring is compressed, but again a motor driven lead screw is used to input the energy into the system. The compressed spring fires a piston attached to the head of the main chassis of the robot upward and away from the foot.

The final coil-spring-based jumping robot was not originally designed as a jumping robot at all, rather it was designed as a simple 'walking' robot. Named Mini-Whegs^{TM} after the hybrid of wheels and legs it has at its corners, that combine 'simplicity, robustness and reliability to provide a desirable combination of speed, mobility and versatility' (Morrey *et al* 2003). The 9J version of the robot, depicted in figure 1(*c*), is powered by a motor which rotates all four of the 'whegs' at the same time at a single speed. The jumping capability was added to improve its ability to get over larger obstacles. Jumps are achieved by employing a four-bar linkage and coil spring. The spring is stretched using a second motor within the chassis and releases automatically when the spring is fully extended.

2.2. Bending spring based designs

The Scout robot (Stoeter *et al* 2002) was developed as a platform for distributed robotic systems where multiple devices would work in conjunction to achieve a common mission goal. The basic robot is cylindrical with a wheel at each end allowing motion on smooth surfaces and is shown in figure 1(*d*). For jumping, a steel spring foot is bent by a winch and cable, thus storing energy for a subsequent jump.

2.3. Fluid powered designs

Researchers at the Sandia laboratories developed the Sandia hopper (Weiss 2001) pictured in figure 1(*e*). Utilizing the combustion of liquid propane to fire a piston into the ground, jumps can be achieved through the acceleration of the heavier upper body. The device jumps semi-randomly making general progress in the required direction rather than accurate progression from one point to another. The hopper adopts a weighted self righting system (not pictured) and a steering system that takes a bearing from an internal compass before moving an off-centre control mass which tilts the device in the intended direction of the jump.

The second fluid-based jumper uses the expansion of compressed air to rapidly fill and extend pneumatic cylinders. The Tokyo Institute of Technology 'Airhopper' (Kikuchi *et al* 2003), shown in figure 1(*f*), has a tubular body with four widely-spaced legs providing a stable platform. Each leg consists of a four bar linkage driven by a pair of pneumatic cylinders.

2.4. Momentum-based designs

At the time of writing only one robot uses momentum to initiate a jump. When a human jumps vertically, as well as compressing the legs which release most of the jumping energy, the arms are also swung upwards in a pendulum fashion

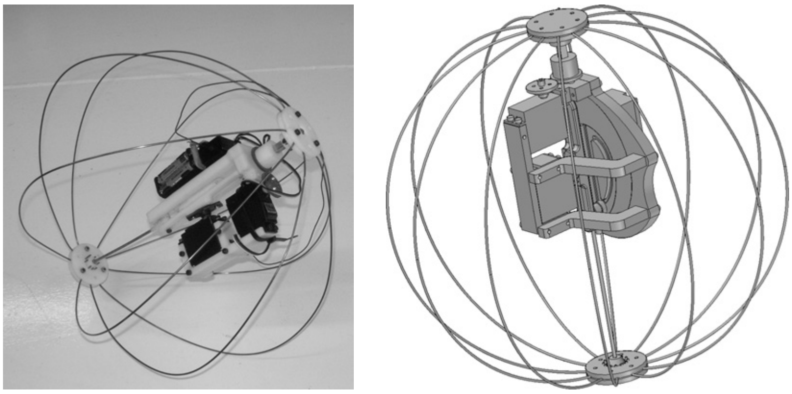

(*a*) (*b*)

Figure 2. (*a*) Photograph of Jollbot, (*b*) CAD model of Jollbot.

to improve the jump height. A number of papers suggest that the arm swing improves vertical jumping performance in humans by around 10% (Vanezis and Lees 2005). The team at Kagoshima university have used this phenomenon to develop a pendulum jumping machine (Hayashi and Tsujio 2001). By swinging a servomotor actuated arm, the machine is able to make a small vertical jump. A forward jump has been difficult to reproduce with a single pendulum, but a robot with multiple counter-rotating pendulums has successfully climbed small steps.

2.5. *Elastomer-based designs*

The department of robotics at Ritsumeikan University in Japan has developed a 40 mm diameter tethered deformable robot that can roll and jump using shape memory alloy (SMA) spokes within a soft rubber shell (Sugiyama and Hirai 2004). When a voltage is applied to the SMA spokes they contract, moving the centre of mass of the robot towards the rubber hoop. By controlling which SMA actuators contract and when, the entire robot is able to roll along. The rubber element acting as the tyre for this wheel-like structure is integral to its ability to jump. To jump, the SMA actuators contract on one half of the wheel causing the rubber wheel to buckle. As the SMA actuators begin to extend, the rubber wheel rapidly returns to its original form launching the device into the air as shown in figure 1(*g*). A spherical robot is also being developed to experiment with the possibility of three-dimensional motion.

3. Requirement specification

In addition to the typical engineering requirements, such as manufacturability and cost minimization, several specific requirements for a biomimetic jumping robot are highlighted in table 1, together with their biological justification.

4. New designs

The two designs presented below were developed by the authors of this paper as potential approaches to traversing irregular terrain. In each case, a novel jumping mechanism has been developed based on the biomimetic design requirements specification given above, although both store energy in their respective forms of metal springs for instantaneous release.

4.1. *'Jollbot'*

The main skeletal structure of this robot comes from the metal semi-circular hoops. These hoops are the springs that provide the energy for jumping and make up the outer rolling surface. By compressing the sphere along a central axis joining the nodes/mounting points of the hoops, energy is stored within this outer structure. If this energy is rapidly released then the device will jump in the direction of the axis assuming that there is no slipping at the ground contact point. Direction control of the jump is achieved by adjusting the centre of gravity (CofG) of the device slightly leaning the axis over before launch. A photo and CAD model of the device is shown in figure 2 and the jumping procedure for the device is shown pictorially in figure 3.

Rolling is achieved by orienting the central axis parallel to the ground, and adjusting the centre of gravity of the sphere. Direction control of rolling is possible by moving the centre of gravity out of line with the ground contact area. This is summarized in figure 4. Having an entirely driven outer surface of the device would help it cover uneven terrain and the low ground contact pressure would enable it to traverse soft surfaces such as sand, snow or brush.

The combined jumping and rolling motion results in its name—Jollbot.

4.1.1. Additional requirements. In addition to the general design requirements for an autonomous jumping robot (table 1), the design of this robot considers those requirements relating specifically to rolling, which are shown in table 2.

4.1.2. Design detail. The first design requirement is that the robot must be able to ready itself for a jump using a locally available energy source. Jollbot is powered by a 4.8 V 600 mA h battery pack which supplies two 4.8 V standard model servos and a radio control receiver. The servos,

Table 1. Requirement specification based upon biological inspiration.

Biological inspiration	Design requirement
Animals must eat in order to convert and store the energy required by its muscles for locomotion. The food resources available are generally of a lower than necessary energy density. It was shown in the introduction that power is the performance limiting factor in small jumping animals and insects, for which the specific energy available from muscle contraction alone is insufficient. Power amplification is achieved by operating their muscles at lower than maximum speed, and storing the energy for rapid release.	In order to be fully autonomous, the robot must be able to ready itself for a jump using a locally available energy source.
Different animals store energy in different ways. For example, fleas and leafhoppers store energy in resilin, a rubber-like material, in compression. Larger mammals, such as humans and dogs, store energy in tension in tendons, primarily made from elastin, another material with rubber-like properties. Locusts, however, store their energy in harder skeletal cuticle, in bending.	Energy should be stored somehow, ready for a jump when instantaneous release is required.
Most jumpers have relatively long jumping limbs.	A long leg length (relative to overall robot size) should be chosen for further power amplification.
The large jumping (metathoracic) legs of the locust, for example, are held in the flexed position by a natural catch caused by a belt of tendon becoming hooked around a lump of cuticle (Bennet-Clark 1975, Brown 1967, Heitler 1974). Fleas also rely on a mechanical catch.	A catch mechanism is required to ensure that the robot can remain in the charged condition until its next jump without requiring additional energy to hold it there.
Even the most primitive insects are able to orientate themselves prior to jumping to ensure that they jump away from the ground. Locusts, for example display little or no control on landing, and were frequently observed landing on their heads by one author (Paskins 2007). However, they can quickly find their feet and jump again almost immediately if necessary.	The robot must jump upwards no matter which orientation it lands in.
For an organism to jump, a suitably massive element of its body needs to be accelerated away from the remaining mass. By considering conservation of momentum and neglecting losses, greatest jump height is achieved by maximizing the ratio of the accelerated mass to trailing mass which directly increases take-off velocity.	During jumping, the robot must maximize the ratio of the accelerated mass to trailing mass.
Most animals deliberately jump in the direction that they would like to travel and naturally it would be useful if the robot could do likewise.	The robot must be able to orientate itself prior to jumping.
The additional mass of the required payload would be relatively less detrimental to the peak jump height of larger animals.	The robot must be able to carry a useful payload, such as an environmental sampling device.
In animals, such as humans, it is essential to the preservation of life that delicate organs are protected from excessive impact during locomotion. Connections are not rigid, so forces are damped by these softer tissues. Some animals, such as flying squirrels, are able to glide, enabling them to reduce their landing impact forces aerodynamically.	The robot must be able to carry any sensitive electronic equipment without it sustaining any damage during the jumping and landing cycles.

which have been modified to allow continuous rotation, have integral gearboxes allowing sufficient torque to be developed for storing the jump energy within the hoop springs, and for rotating the slightly off-axis centre of gravity for jump steering and powered rolling control. As jump energy is stored in the hoop springs, it is possible to compress them slowly using a low power source. Jollbot cannot be powered by a locally available energy source as it is currently designed but it may be possible to use photovoltaic cells incorporated into a skin covering the device.

The second requirement states that jump energy should be stored, ready for instantaneous release when required. The metal hoop springs allow energy to be stored in a stable material that is unaffected by stress-relaxation. The spherical form of the robot allows pre-stressed spring elements to be used thus enabling more energy to be stored for a given displacement than would be possible to standard unstressed springs. Jump energy is stored in the hoop springs by a centrally mounted compression mechanism. The compression mechanism sits on a chassis which is fixed to the top or

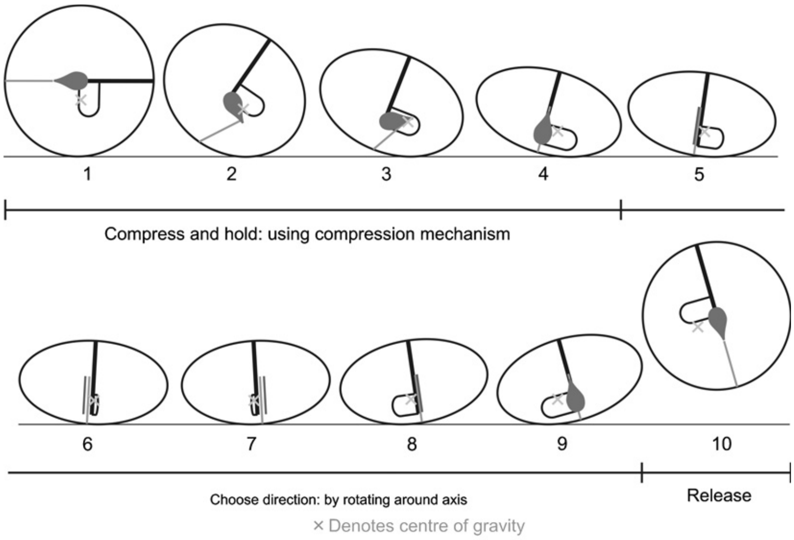

Figure 3. Jumping methodology for Jollbot.

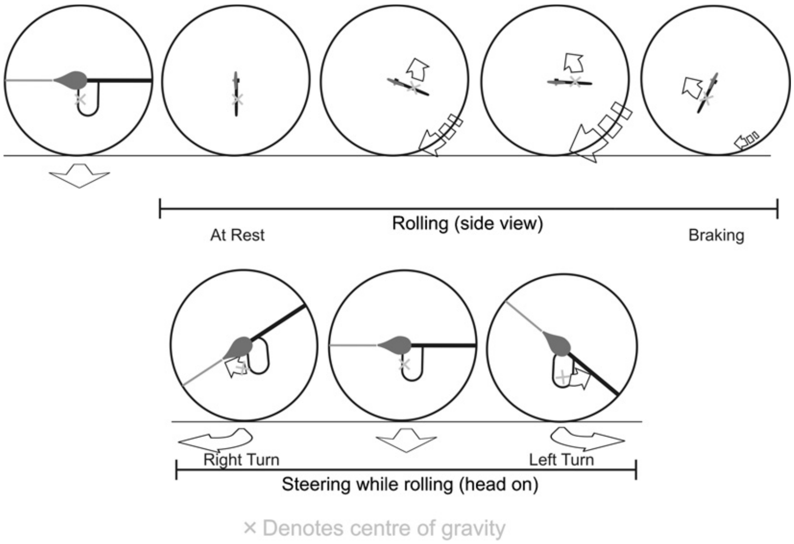

Figure 4. Rolling methodology for Jollbot.

Table 2. Additional design requirements based upon biological rolling.

Biological inspiration	Design requirement
The Web-toed Salamander (Garcia-Paris and Deban 1995) and Namib Golden Wheel Spider (Henschel 1990) form wheel-like shapes to enable them to roll passively down sloping surfaces more quickly than would be possible by running. Tumbleweed (Antol *et al* 2003) is able to cover many miles of comparatively flat surfaces being driven solely by the wind. The slight bouncing motion caused by its off-centre centre of gravity (CofG) enables it to roll over small obstacles.	Robot should be able to roll passively.
Only two animals are able to 'roll' using their own physiology for power—the Mother-of-Pearl Moth caterpillar (Brackenbury 1997), and the stomatopod shrimp, Nannosquilla decemspinosa, (Caldwell 1979, Full *et al* 1993)—both of which can semi-continuously roll along flat and upward sloping surfaces by adjusting their centre of gravity within a wheel-like form.	Robot should be able to roll actively.

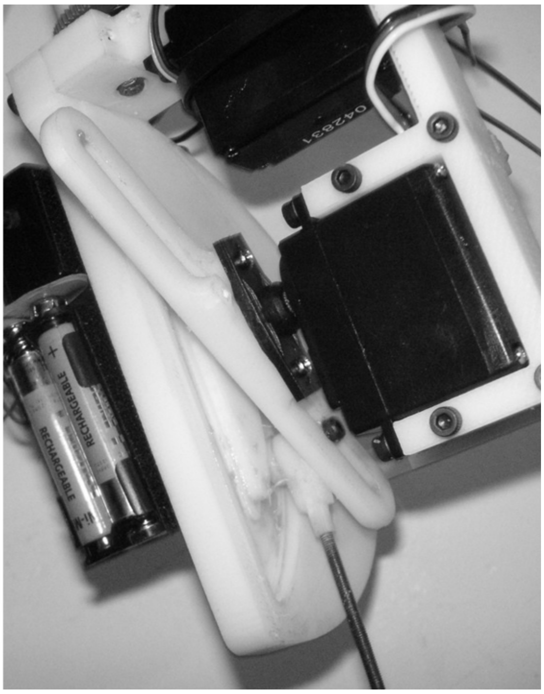

Figure 5. Photograph showing detail of guide, face cam and slider roller in Jollbot.

'head' of the robot, and consists of a model servo rotating a continuously variable length crank connected directly to the 'foot' at the opposing side of the sphere. As the servo rotates, the head and the foot of the robot are pulled together storing energy in the springs.

The variable length crank mechanism was developed after initial testing with a simple fixed length crank with an over running one-way clutch mechanism. To maximize the stored energy, the compression system, powered by a constant-torque motor, should adapt to the required compression force. As the hoop springs are compressed, the force required increases with displacement. Therefore, when using a fixed length crank the required rotary torque increases as the deflection increases. By introducing a crank that varies in length as it rotates, the output force can vary while the input torque remains constant. This has been achieved by using a guide, face cam and slider roller as shown in figure 5. This revised mechanism outperformed the fixed length crank mechanism since it is able to compress more hoop spring elements using the same model servo. Unfortunately, the mechanism substantially increased the overall weight of the device; however, it is not yet fully optimized.

As the motor rotates the guide, the face cam ensures the slider roller moves in a specified path and therefore at a variable crank length around the servo axle. The face cam was designed to be replaceable for tuning purposes. The cam that finally worked the best kept the slider roller at a constant radius for a short time slowly compressing the sphere. As the guide rotates towards 90°, the radius of the cam reduces slightly, and between 90° and 180° rotation the radius reduces further to ease the loading on the motor. As soon as the 180° position is reached, the slider roller is free to move in the axial direction because of the cam profile and the slot along the guide. This straight axial release of the spring energy ensures that none is wasted unnecessarily as would be the case with a rotating fixed length crank. The guide then continues to rotate beginning another energy storage phase. Figure 6 shows a pictorial representation of the compression phase of Jollbot, illustrating how the crank length continuously varies throughout the rotation of the servo. This whole process takes 1.44 s which is comparatively slow compared to the release phase which takes only 0.24 s as shown in figure 7.

The third requirement relates to maximizing leg length to further improve power amplification. Although Jollbot has no 'legs' in the traditional sense, the effective leg length is approximately one quarter of the diameter of the sphere since that is the length through which the robot travels before takeoff. With optimization, it should be possible to increase this length to around half the diameter of the sphere but without

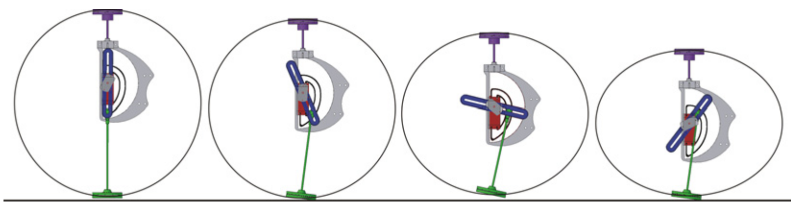

Figure 6. Pictorial representation of the compression phase of Jollbot.

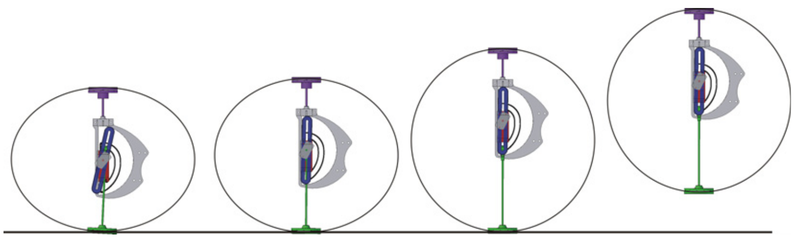

Figure 7. Pictorial representation of the jumping phase of Jollbot.

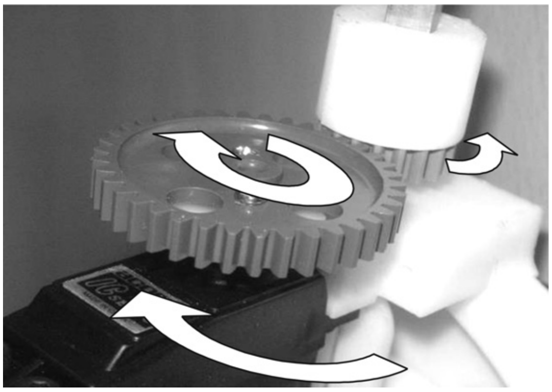

Figure 8. Jollbot jump direction and rolling mechanism.

significant re-design of the compression mechanism, this ‘leg’ length cannot be increased further.

The fourth design requirement states that a catch mechanism is required to ensure that the robot can remain charged until its next jump without requiring additional energy to hold it in that position. Jollbot has a simple catch mechanism which relies on an unstable equilibrium point at complete compression and just before release. With the current manual remote control system, it proved very difficult to stop the mechanism at the required point on the cam.

The fifth design requirement says that the robot must jump upwards no matter which orientation it lands in. This is only achievable with careful control and positioning of the centre of gravity within the spherical shape of Jollbot. The centre of gravity was estimated by suspending the device on threads secured at various points. The CofG is inline and below the thread, so by combining images of the device hanging in different orientations the CofG can be found. In its current iteration, Jollbot’s centre of gravity lies slightly towards the ‘head’ of the robot which results in toppling upon landing, from which it is not possible to recover. If the centre of gravity was slightly below the equator line, perhaps by adjusting the position of the battery pack, then Jollbot would always roll onto its ‘foot’ after a successful jump.

The sixth requirement states that the ratio of accelerated mass to trailing mass should be maximized. This is achieved by attaching the relatively heavy main chassis, consisting of the compression and steering mechanisms and motors, directly to the head of the robot.

The seventh design requirement relates to the direction control of jumps. By releasing jump energy at an angle to the vertical, it should be possible for Jollbot to make projectile jumps. Jump direction is controlled by rotating the slightly off-axis centre of gravity around the head-foot axis using a second model servo. The servo is mounted onto the main chassis and drives itself around a gear fixed to the spherical shell of the robot as displayed in figure 8. This enables the entire central chassis and its associated components to twist, adjusting the centre of gravity and therefore the lean of the main jumping axis. The semi-spherical form of the foot and hoop springs when compressed allows the robot to lean in any direction as shown in the video stills in figure 9. Full testing of this jump steering mechanism was not undertaken since it proved difficult to control both servos accurately to ensure the ‘compress and hold’, ‘choose direction’ and ‘release’ stages occurred in series. The absence of a stable catch, as discussed above, was the main contributing factor.

This same jump steering mechanism is also intended as the powered rolling mechanism for travelling along level surfaces, over small obstacles, and even up sloped surfaces. Since the centre of gravity does not lie exactly along the head-foot axis, rotating the chassis around the axis should move the centre of gravity outside the area of contact of the hoop springs with the ground. This mechanism did not perform as anticipated since the area of contact was too large with the few hoop springs

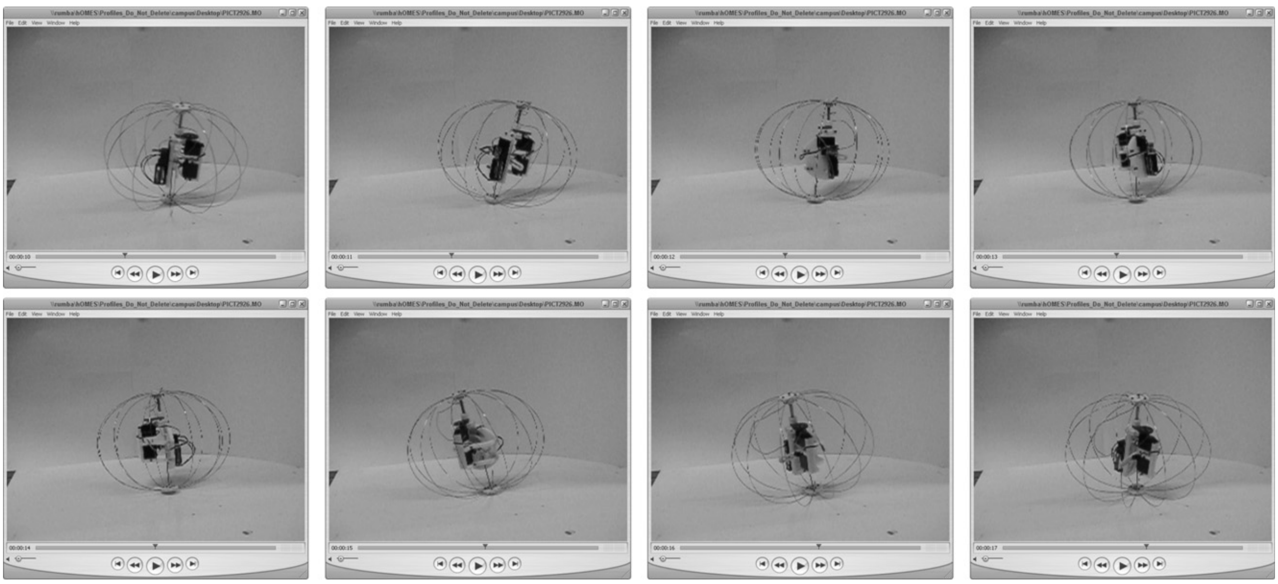

Figure 9. The jump direction control of Jollbot.

on the device. The axial location of the centre of gravity also meant that keeping the axis horizontal for rolling was very difficult.

The presented Jollbot device does not have any provision for direction control whilst rolling because steady-state rolling was initially more important. Tilting the internal axis from its normal horizontal position would cause the robot to lean over and make gentle turns in the direction of the axis tilt.

Due to the spherical shape of the robot, Jollbot will passively roll down surfaces, and bounce off obstacles, particularly after a jump. The spherical form also ensures that there are no body extremities that can get caught on obstacles. The springs on its outer surface will also absorb much of the impact energy from collisions and landing, thus protecting sensitive equipment from damage. However, if the robot were to land directly on its 'head' then the chassis would take much of the impact force but it is felt that that would be an uncommon occurrence. If the robot were covered with a suitable skin, then complete environmental protection may be achievable for all internal components. These internal components would include the electronics and control system required for autonomy consisting of elements such as position and ranging sensors, a vision system, environmental energy recovery system, data logging or transmitting equipment, amongst others. A stable non-rolling platform is possible at the transition between rolling locomotion and a jumping one for assessment of the area surrounding the robot. Jollbot could carry additional payloads with an expected reduction in jumping performance, but it has the benefit that they will be enclosed within a safe structure.

4.1.3. Robot performance. In order to measure the jumping performance of the robot, a Redlake Images Motionscope high-speed camera was used to film each jump at pre-selected frame rate. Scion Image (useful internet freeware that can handle sequences of images, and output the pixel coordinates of all the points clicked on by a user in order, www.scioncorp.com) was used to determine the height of the different components of the robot in each frame. In order for this method to be valid, the robot was always placed such that it jumped in the plane parallel to the camera lens, and both a horizontal and a vertical calibration performed using graduated markers.

The jumping performance of the 0.3 m diameter Jollbot is illustrated in the high speed camera images in figure 10 taken at a rate of 50 Hz. From the images, it was determined that the robot raises its centre of gravity by 218 mm through the course of the jump, which is approximately 2/3 its entire height. It can clear a height of 184 mm.

The efficiency of various mechanisms within the robot can be determined by comparing the energy of the device in different states. A comparison between the electrical energy consumed and the energy stored within the system gives a conversion efficiency for the compression mechanism. Comparing the energy stored with the potential energy of the robot at peak height illustrates the efficiency of the release mechanism.

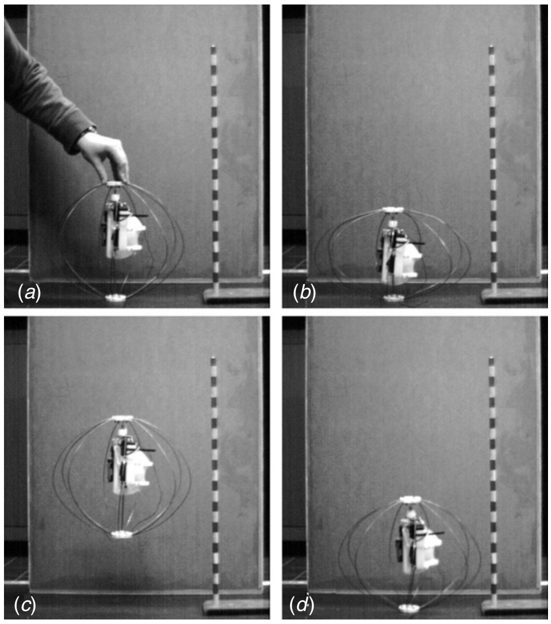

Figure 10. High speed camera images illustrating the jumping performance of Jollbot: (*a*) resting state of Jollbot, diameter = 294 mm, (*b*) 1.44 s later, Jollbot is ready to jump after compressing 65 mm, (*c*) 0.24 s later, Jollbot is at its peak jump height, clearing 184 mm, (*d*) 0.22 s later Jollbot hits the ground and absorbs impact energy in the slight compressing of the sphere.

The electrical energy consumed is found from (9):

$$\text{electrical energy(J)} = \text{voltage(V)} \times \text{current(A)} \times \text{time(s)}. \tag{9}$$

The potential energy stored in the jumping system is equivalent to the area under a force-displacement curve.

The potential energy stored in a mass suspended at a height is defined in (10) where; m = mass (kg), g = acceleration due to gravity (m s^{-2}), h = change in height of CofG (m).

$$PE = mgh. \tag{10}$$

In Jollbot's case, the servo draws a peak current of ~1.2 A from the 4.8 V battery pack over the 1.44 s compression. From (9), this gives a total energy consumption of 8.3 J. Since the current increased throughout the compression, it is felt that this is far larger than the actual energy consumption and logging of the current values throughout the short compression time would give a more accurate value.

The energy stored within the robot's spring system was estimated from the area under a force displacement curve produced through testing on an Instron compression testing machine. This resulted in approximately 1.1 J of stored energy.

The potential energy of the device was determined using (10), where the mass of the robot is 0.465 kg and the change in height of the CofG is 0.218 m. This results in 1 J of potential energy.

Comparing the first two energy measurements with one another, results in a conversion efficiency of 14% for the compression mechanism. Comparing the second two energy measurements results in a mechanism release efficiency of 91%.

Table 3. Additional design requirements based upon biological gliding.

Biological Inspiration	Design Requirement
Flying squirrels have been observed to fully abduct their limbs during take-off, deploying their gliding membranes, patagia, in the process. This behaviour occurred even during leaps when it was demonstrated that the squirrels achieved no resultant advantage in landing altitude (Paskins *et al* 2007).	The robot should have membranous wings to enable gliding, and these should deploy automatically and fully during take-off.
Flying squirrels choose to pitch upwards immediately prior to landing, rapidly increasing their angle of attack in order to reduce impact forces (Paskins *et al* 2007). Likewise, flying fish deliberately employ air braking to slow themselves down prior to re-entering the water, by positioning their pelvic fins forwards, and angled against the motion (Davenport 1994).	The robot should have the ability to control its angle of attack during the gliding phase to enable effective air braking as it lands.

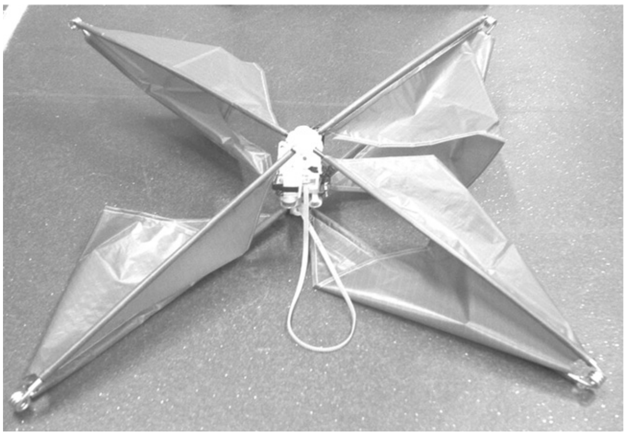

Figure 11. Photograph of Glumper winding itself in, taken immediately prior to take-off.

4.2. 'Glumper'

The concept behind Glumper was for a robot which would jump and then glide, in the hope that this would simultaneously extend range and reduce impact forces. As such, two further biomimetic requirements specifications are shown in table 3 as they are only relevant to Glumper.

The photograph of Glumper (figure 11) shows its four long legs, each with a torsion spring 'knee' at its midpoint, distributed perpendicularly between a 'head' and a 'foot'. A triangular shaped membrane mounted between each leg element and along the axis of the robot acts as its gliding wings. By way of introduction to some of the more complex design solutions, an overview of the discrete steps required for Glumper to jump is given in figure 12.

4.2.1. Design detail. The first requirement specified for this robot was that it must be able to ready itself for a jump using a locally available energy source. Small motors can still generate relatively high torques with sufficient gearing, which is ideal for autonomous applications where the time taken to charge the jumping mechanism is of secondary importance to the maximum achievable performance. Next it was specified that energy should be stored somehow and instantaneously released into a jump. Although elastomers have the capacity to store a lot of energy, this property is severely affected by temperature and time. In the loaded state, energy is lost with time due to stress–relaxation and at cold temperatures, rubber-like materials become hard and brittle, causing them to fail before much energy has been absorbed. The time taken to charge the robot is likely to be long, and extreme environments present the most useful applications for a jumping robot, so storing energy in bending should provide a more suitable approach. Therefore, Glumper stores energy in the compression of four heavy-duty torsion springs, made from $3\frac{3}{4}$ turns of 4 mm diameter spring steel rod, which are mounted in the knee-like hinge-joints of its four legs.

A long leg length (relative to overall robot size) was specified to amplify the power produced by releasing these compressed torsion springs. Glumper's legs are each made from two hinged carbon-fibre reinforced plastic (CFRP) rods, 0.5 m long and with very high specific stiffness so that they almost fully compress the torsion springs without bending themselves. If it required less force to bend the legs than to

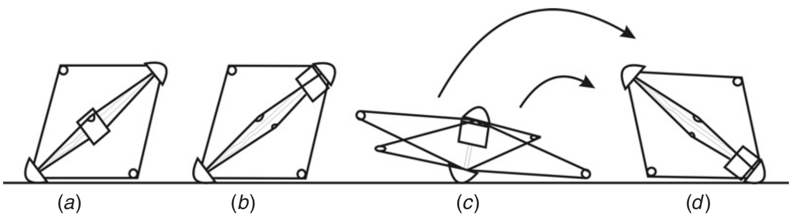

Figure 12. A sketch to introduce the steps required for compression and release of Glumper, showing (*a*) a mechanism is freely suspended on a cord between the head and the foot, which can wind in the cord to compress the robot. (*b*) This compression mechanism can be attached to whichever end of the robot is uppermost. (*c*) When the robot becomes fully compressed a clutch releases the cord and the robot jumps upwards. (*d*) After landing the clutch requires resetting and the process can repeat. The gliding membranes are omitted for clarity.

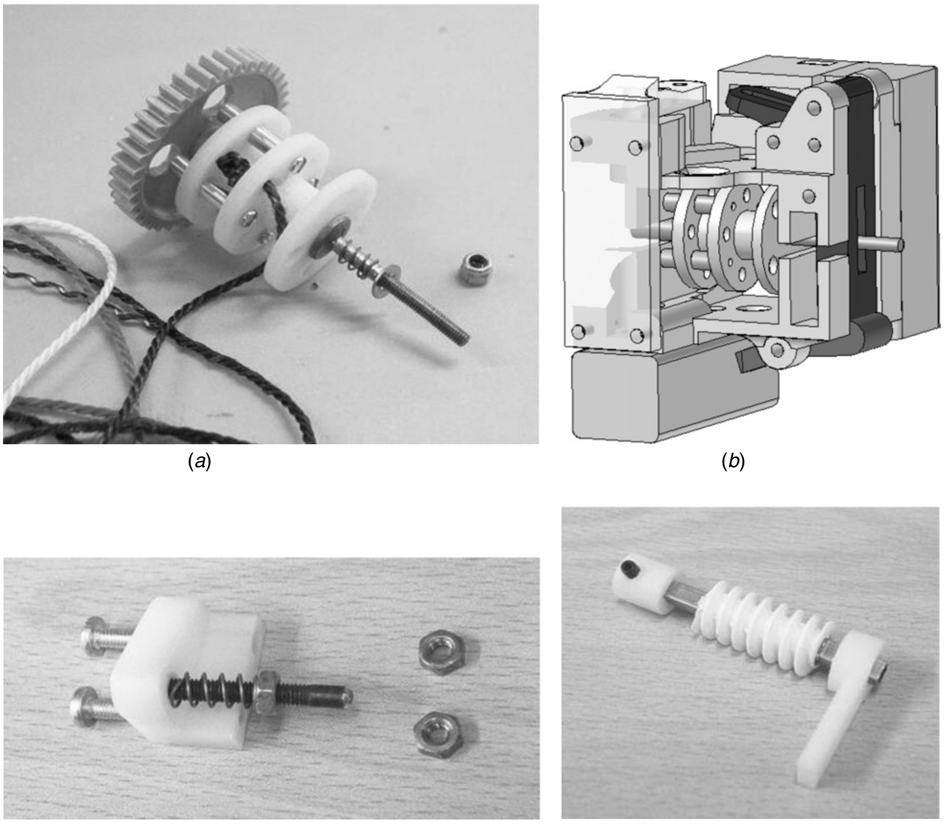

Figure 13 panels: (*a*) (*b*) (*c*) (*d*)

Figure 13. (*a*) Photo of the capstan shaft assembly, showing how it is driven by locating bolts through the drive gear on the left of the image, and the compression spring against which it can be released by pulling on this stepped shaft. (*b*) Rendering from Solid Edge v.17 of the control box showing the hinged lever (the darkest shaded component) and its retaining clip beneath (highlighted in a slightly lighter shade). Some components, such as the bi-stable mechanism and the gears have been omitted for clarity. (*c*) The bi-stable mechanism, consisting of a compression spring, a nut and bolt with a hemispherical end. (*d*) The worm gear sits on a brass square-section drive shaft, but is free to move along the axis such that rotation in one direction pushes the follower (shown on the right of the image) and the reverse direction turns the capstan driving gear shown in (*b*).

compress the springs, the total energy stored would be less once the robot had reached full compression.

The mechanism to allow steady compression and rapid release of Glumper is comparable to a dog clutch. A capstan gradually winds in a loop of cord which passes through both ends of the robot in order to compress it. The capstan is free to rotate on the narrow section of a stepped shaft, between the step and a circlip. Normally a compression spring on the shaft pushes against the circlip to keep some protruding rods from the capstan engaged with corresponding holes in its drive gear (which sits on the thicker section of the same shaft). Thus the capstan can be disengaged by linear actuation of the shaft, allowing the cord to unwind rapidly under the tension of the compressed robot. The capstan drive gear is turned by a worm gear that is forced to rotate by a small motor, but is free to float axially between two points to perform a secondary function that will be discussed shortly. Another advantage of using a worm gear to drive the capstan is that, in the event of power loss, the robot will remain in its partially compressed position because the stored energy does not act directly against the motor stall torque. Such a design is essential for irregular power sources such as solar cells.

The friction acting against the required linear movement of the stepped shaft to push the capstan away from the drive gear is very high when the robot is highly compressed, such that separate linear actuation required for release would need high power. To avoid that problem, a hinged lever automatically pulls the shaft outwards to release the dog clutch when both ends of the robot are pulled in against the control box. Figure 13(*b*) shows a view of the partially complete control box to illustrate how the vertically compressing robot can pull the capstan shaft only when a release latch is moved away from the end of the hinged lever (both components are highlighted in the figure using dark shades). An M3 lock nut must be fitted on the capstan shaft (in order for it to move at all when the hinged lever is depressed), and the position of this nut allows full adjustment of the resultant linear movement of the shaft. A bi-stable mechanism on the hinged lever was necessary to prevent premature re-engagement of the capstan before it is fully unwound. This is due to the compression spring on the capstan shaft. A hemisphere is held protruding into a hole in the side of the closed hinged lever by a stiffer compression spring, such that moving the lever requires significant initial force but once overcome, it moves quickly to the fully open position, being held there by the returning hemisphere. This hemisphere was achieved rather crudely by depositing a solder blob on a sawn off M3 bolt, as shown in figure 13(*c*).

After a jump, the hinged lever needs to be reset in order that winding can be restarted. This is achieved without the need for a separate motor thanks to the ability of Glumper's worm gear to slide along its driveshaft between two physical stops depending on which direction it is driven in. Driving the shaft in one direction causes the worm gear to inch itself along the teeth of the driven gear until it reaches the motor output shaft, after which continued rotation turns the driven gear and hence the capstan. By reversing the direction of the motor, the worm inches itself back along the teeth of the driven gear away from the motor, pushing a recessed follower as it travels. This is guided towards the hinged lever and on contact, this has sufficient force to flip it back past the bi-stable catch ready for the next jump. This 'sliding worm' design requires high friction on the gear driven by the worm, which is achieved by mounting it fairly tightly against the side wall of the control box.

An important advantage of Glumper's design is that any potential payload will not be rigidly connected to the extremities of the robot. By choosing a suitable cord length, it will be slack when released at takeoff, so the time of action of the landing force on the control box increases, and hence the total impulse is lower. Thus the risk of damage to any sensitive electronic equipment within the control box is reduced during the repeated jumping and landing cycles.

This research required a robot with membranous wings to enable gliding, which should deploy automatically and fully during take-off. Deployment of the gliding membranes during take-off avoids any complications that would otherwise be caused by the need to conserve angular momentum in mid-air. Glumper naturally adopts this behaviour because it has four triangular-shaped rip-stop nylon membranes spanning the gap between its legs and the mid-line between the head and foot. The robot should have the ability to control its angle of attack during the gliding phase to enable effective air braking as it lands. The mass of Glumper's compression mechanism is localized in a box which is free to move between its head and foot, so the pitch angle can be controlled by incorporating an additional motor. This drives a pulley quickly along a toothed belt, loosely attached between the head and foot of the robot, thus moving the centre of mass either forwards or backwards during gliding flight depending on motor direction. This design also enables the control box to attach itself to whichever of the two ends of the robot is uppermost in between jumps, so the robot can jump upwards no matter which orientation it lands in, and the ratio of accelerated mass to trailing mass is maximized.

The requirement that the robot must be able to orientate itself prior to jumping could be achieved by rotating an eccentric mass, such as the battery pack, around the control box. The slight protrusion of the head/foot from the legs means that this rotation should cause the centre of mass to shift sufficiently to rock Glumper from a stable position resting on one pair of legs to a stable position on another, but unfortunately no such mechanism has yet been developed.

Although an autonomous control system has not yet been developed, only the direction of Glumper's two lightweight, low power dc motors would need to be controlled at present, and this could be achieved by using a small number of sensory inputs. Ultimately this control system would need to be expanded to include direction control and decision making.

4.2.2. Robot performance. In vertical jump tests, the average change in Glumper's estimated centre of mass between the pre-launch state and the peak height is 1.6 m ($n = 4$, SD = 0.07 m) and its peak clearance height averages 1.17 m ($n = 4$, SD = 0.07 m). In order to determine the efficiency of Glumper's energy storage and release mechanism, the force required to fully compress Glumper was measured using an Instron compression testing machine. From the area under the resulting force–displacement curve, it is estimated that Glumper is able to store 21.5 J of energy. If the launch mechanism was 100% efficient, the maximum height that Glumper could reach can be predicted by assuming that all this energy would be converted to potential energy at the peak of a vertical jump. The total weight of Glumper during testing was 700 g, so a hypothetical vertical increase in the height of its centre of gravity of 3.1 m should be possible, meaning that its energy storage and release mechanism is actually only 52% efficient.

A multi-meter was used to measure the current drawn by Glumper every 30 s during its compression and release. The total time for wind-in using its two rechargeable lithium ion cells (wired in series with an operating voltage of 8 V) is 435 s. The current rises steadily, rising sharply just before take-off when it reaches 0.4 A, equivalent to a peak electrical power requirement of 3.2 W. Solar power is an example of a locally available energy resource for many potential robot applications. On Earth the Sun's radiation is diffused and scattered by the environmental conditions, reducing the maximum power delivered from the 1370 W m^{-2} available in space at the radius of the Earth's orbit. Photon Technologies Powerfilm® flexible solar modules are specified as generating 0.15 W each of power in bright sunlight for a panel of 15 × 3 cm (Photon Technologies, Colorado Springs, CO, USA). Their flexibility, low weight and size would make them ideally suitable for mounting on Glumper's membrane wings. Importantly, only two wings could ever be directly pointing at the sun irrespective of robot orientation, which is enough area for 45 panels. Hence, a maximum power of 6.75 W is theoretically available and Glumper's control mechanism thus satisfies the requirement that it should be able to ready itself for a jump using a locally available energy source. By plotting the electrical power against time, the total electrical energy required to power a jump (the area under this curve) was estimated to be 80.5 J. Therefore, the efficiency of the conversion of electrical energy into strain storage energy is approximately 3.3%, with some of this deficit clearly being converted into heat.

The effect of reducing mass on jump height was demonstrated in an experiment using the Glumper robot without its control box. The mass of this structure including the foot, legs and springs was 375 g. Various weights were added

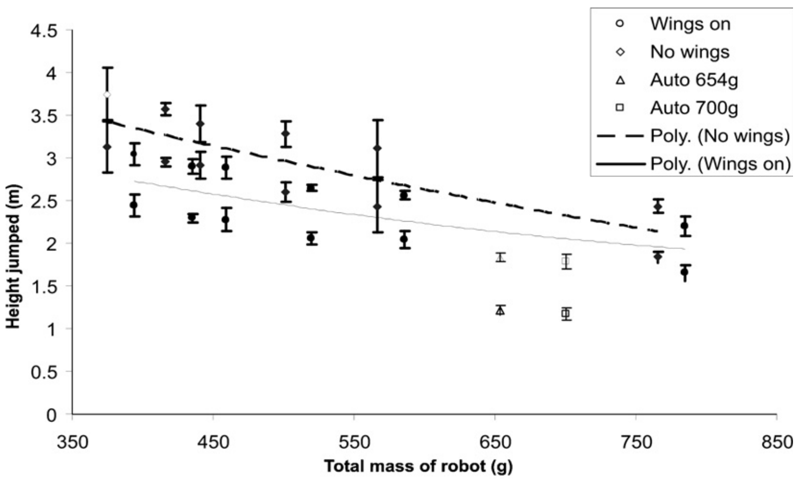

Figure 14. Graph showing that adding mass to Glumper's basic frame reduces its peak clearance height both with and without its wings attached. The graph was produced by measuring the peak height of both the head and foot of the robot repeatedly for every given condition, and plotting the average values. Microsoft Excel was used to plot a polynomial trendline through the centre of these head and foot points for both the winged and non-winged measurements, and the respective equations of the resulting curves are displayed. The average height of Glumper's head and foot for automatic launches is shown for comparison, powered by one (654 g) and then with two onboard lithium cells (700 g). The error bars represent ±1 standard deviation from the means in all cases.

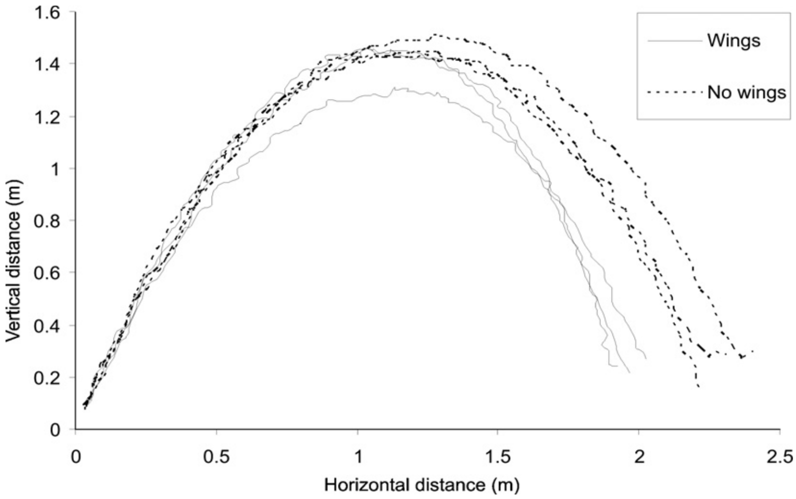

Figure 15. Graph showing the trajectories followed by Glumper's centre position when launched automatically at an angle of 63° to the horizontal, with and without its membranous wings.

to its head before manually compressing it and launching it vertically. A ruler was used to ensure that the robot was always compressed such that there was a 10 cm gap between the head and the foot, which is equivalent to how much it compresses when launched by its automatic launch mechanism. The results are shown graphically in figure 14, and it can be seen that the optimum total mass of the robot would be less than its current frame weight. No momentum advantage would be gained by adding mass to the current control box to improve the ratio of accelerated to trailing mass of the robot. Glumper's total mass was 700 g, including its four wings, which in total weigh 19 g. One of the initial requirements was that the jumping robot must be able to carry a useful payload, such as a camera and transmitter for example. Figure 14 demonstrates that it should be able to absorb the additional weight of the example payload, perhaps 50 g, without a large decrease in jump height.

It can be seen from figure 14 that more energy is lost when Glumper launches itself automatically, which is likely due to friction as the cord unwinds from the capstan. It is also clear that the wings cause a reduction in peak jump height, presumably owing to air resistance.

Figure 15 shows the trajectories followed by Glumper's centre position during six jumps launched automatically at an angle of 63° to the horizontal, three with and three without its membranous wings attached. The presence of the wings actually reduces the total range of the jump rather than extending it as was intended. This might change with weight reduction, which should simultaneously improve peak jump height and the lift to drag ratio during gliding. However, the reverse may also be true because air resistance against the wings would also be relatively more effective acting against the ascending robot. Unfortunately it has not been possible to test the effect of altering Glumper's pitch angle, while gliding, to the resultant trajectory because a suitable control system was never developed, and the flight time was typically short prohibiting remote control.

5. Discussion

Table 4 compares the performance data of Jollbot and Glumper with equivalent data for the existing jumping robots introduced previously in order to facilitate the evaluation of the two new designs. The maximum jump height for each robot is assumed to be the change in height of its centre of gravity between the pre-launch state and its peak height. It is important to consider that the other robots were not developed using the biologically inspired design specification presented in this paper and may have had other objectives.

The definition of the performance of a jumping robot depends entirely on the specific requirements of an application. Here we have chosen to evaluate the robots above based on a space exploration application no matter their actual intended application. Surface exploration of other planets requires that the robot is able to move across rough terrain, so the robot should jump over the largest possible obstacle, whilst also being of the smallest possible volume to ensure that it takes up as little room as possible in the launch craft. Being of small size also means that many can be sent in place of a larger exploration rover, or that one robot could be used in conjunction with other exploration devices.

Figure 16 is adapted from (Bennet-Clark 1977) and shows jump height against object length for all of the robots reviewed including some data on animals for comparison. An assumption is made that all animals and robots presented here can only accelerate through a distance equal to their leg length. Owing to the fact that all the animals and robots presented here have similar aspect ratios, body length becomes an acceptable measure of both leg length and object size. The horizontal lines show energy density and the sloping lines are a measure of power per unit weight, derived from (8). The power to weight ratio of direct muscle action in animals has a practical limit of 100 W kg^{-1} (Bennet-Clark 1977). Hence, all the animals above that line in figure 16 are producing more power than their muscles can deliver, indicating some additional energy storage mechanism.

Optimal performance of a jumping robot for use in planetary exploration was declared to require maximization of height together with minimization of mass and volume to reduce the cost of space transport. Considering figure 16, the closer the robot sits to the top left corner of the chart, the better. This is equivalent to a maximization of power density, represented by the diagonal lines, which is consistent with the statement in the introduction that decreasing size demands increased power to achieve equivalent height.

Glumper achieves a superior power density to Jollbot. The power density of approximately 20 W kg^{-1} achieved by Jollbot is also inferior to that of all the natural examples displayed.

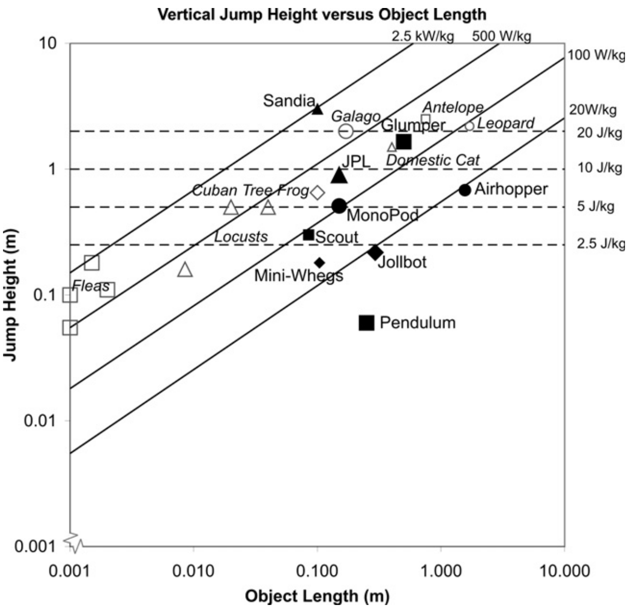

Figure 16. Height of jump versus length of a selection of animals (outlined markers) and robots (solid markers). The graph also shows required specific energy and specific power required to produce a jump assuming that the objects accelerate through their own body length and that there is no air resistance.

Looking parallel to the lines of power density in figure 4, Glumper has comparable performance to the animals that would not be considered to be specialized jumpers, sitting directly between the domestic cat and the antelope. The jump heights recorded by specialized jumpers, such as fleas, frogs and the lesser galago all demonstrate a superior power density.

In terms of both power density and energy density, Glumper outperforms all the documented jumping robots in figure 16 with the exception of the Sandia robot, which is propelled by the combustion of propane. This superior performance would be expected because the energy density of hydrocarbons is much higher than that of springs, and the authors can think of no comparable biological transport modes. The use of combustion to power jumps was not considered in this research, due to the primary requirement of autonomy. Other potential applications are also prohibited by this design. In confined areas, for example, exhaust gases could pose a problem and on other planets, the lack of oxygen in the atmosphere would prevent the burning of fuel (though high explosives could obviously be used). Springs are the next best energy storage medium, because the robots with either helical or bending springs, including Glumper and Jollbot, outperform the remaining devices. This does not even take into account that those devices, Airhopper, Pendulum and Deformable all rely on external power giving them an immediate weight advantage. It is also clear from figure 16 that Jollbot was outperformed by other robots with equivalent energy storage mediums. It is not clear from this sample whether one type of metal spring consistently outperforms any other although no difference was expected. The only elastomer-based jumping robot does not jump particularly high, but the absence of other published devices storing energy

Table 4. Robot details and jumping capability.

Robot	Energy storage medium	Jump height (m)	Jump distance (m)	Weight (kg)	Size $L \times W \times H$ (m)	Control	Power source	Jump steering method
JPL Hopper (V2)	Metal helical spring	0.9	2	1.3	$0.15 \times 0.15 \times 0.15$	Radio controlled	Onboard batteries	Rotating foot
Monopod	Metal helical spring	0.51	0.305	2.4	$0.15 \times 0.2 \times 0.3$	Autonomous (from IR sensors)	Onboard batteries	Rotating foot
Jumping Mini Whegs	Metal helical spring	0.18	Not known	0.191	$0.10 \times 0.08 \times 0.05$	Radio controlled	Onboard batteries	Turning robot before launch
Sandia	Fluid powered	3	3	2.5	$0.1 \times 0.1 \times 0.2$	Follows built-in compass	Liquid propane	Moving centre of gravity
Airhopper	Fluid powered	0.68	0	20	$1.5 \times 1.1 \times 0.5$	Remotely controlled via cable tether	External compressed air supply	(Not possible unless legs ‘walk’)
Pendulum	Momentum	0.06	0	0.72	$0.25 \times 0.1 \times 0.25$	Remotely controlled via cable tether	$\sim$9 V power supply	No steering possible
Deformable	Elastomer	0.08	0	0.003	$0.04 \times 0.02 \times 0.04$	Remotely controlled via cable tether	External power supply	(Not possible unless spherical)
Scout	Metal bending spring	0.3	0.25	0.2	$0.09 \times 0.11 \times 0.05$	Radio controlled	Onboard batteries	Turning robot before launch
Jollbot	Metal bending spring	0.218	0	0.465	$0.3 \times 0.3 \times 0.3$	Radio controlled	Onboard batteries	Moving centre of gravity
Glumper	Metal bending spring	1.6	2	0.7	$0.5 \times 0.5 \times 0.5$	Manually activated	Onboard batteries	Not implemented

in elastomers was unexpected. This may be due to the gradual loss of energy resulting from stress relaxation during the pause inherent in a pause-and-leap robot.

Power density can be increased by either increasing power or reducing mass. More power can be produced by generating higher force or reducing its time of action over a given distance. In animals this is limited by the maximum power output of muscle resulting in the use of energy storage. Therefore the performance limiting factor for a jumping robot is its energy storage and release mechanism. The mass reduction experiment conducted on the Glumper robot demonstrates clearly the advantage of reducing unnecessary weight. It is possible to eliminate mass from engineering systems through optimization techniques such as FEA and by changing materials, whereas nature's jumpers are already highly optimized as a result of natural selection. The Sandia robot has already proved that it is possible to outperform nature's jumpers by using a hydrocarbon-based energy storage and release mechanism, which requires the use of high performance materials in its construction. Such materials are unavailable to natural organisms due to other practical constraints, such as reproduction.

6. Future work

It has been shown that the clearance height of the robots in development by the authors could be improved by weight reduction, increasing the force or reducing its time of action.

In the case of Jollbot, although its performance could be improved by optimization of the component materials, it is probable that the performance of this evolution of Jollbot is limited by the design of its compression mechanism, which is unable to produce more force. Specifically, a revised mechanism is being designed to provide greater force and allow for greater compression of the springs. Jumping force will be improved by changing to glass-fibre springs. The poor rolling performance will be improved through the development of a new system allowing for more movement of the centre of gravity of the robot.

Significant size reduction of Glumper's control box is intended by selecting materials with higher specific strength and stiffness. This has the two-fold advantage of weight reduction, and allows additional compression of the robot body so that more energy is stored before release. Clearance height could also potentially be improved by adjusting the attitude of the robot in much the same way as a human high-jumper chooses to pass the bar horizontally. Finally, flexible solar panels should be added to see if the compression mechanism can be powered by these directly, and hence the relatively large mass of the batteries could potentially be removed.

Note. Additional videos and colour images of Jollbot and Glumper are available from the online version of this journal.

Acknowledgment

We would like to give special thanks to the University of Bath and the EPSRC, without whose funding for two of us (RA and KP respectively), this PhD research would not be possible.

References

Alexander R M 1974 Mechanics of jumping by a dog Canis-familiaris *J. Zool.* **173** 549–73

Alexander R M and Vernon A 1975 The mechanics of hopping by kangaroos (Macropodidae) *J. Zool.* **177** 265–303

Allison J 2002 *Monopod Jumping Robot* (Salt Lake City, UT: University of Utah)

Altendorfer R, Moore N, Komsuoglu H, Buehler M, Brown H B, Mcmordie D, Saranli U, Full R and Koditschek D E 2001 Rhex: a biologically inspired hexapod runner *Auton. Robots* **11** 207

Antol J, Calhoun P, Flick J, Hajos G, Kolacinski R, Minton D, Owens R and Parker J 2003 Low cost Mars surface exploration: The Mars Tumbleweed *NASA Report* NASA/TM-2003-212411

Bennet-Clark H C 1975 The energetics of the jump of The Locust Schistocerca Gregaria *J. Exp. Biol.* **63** 53–83

Bennet-Clark H C 1976 Energy storage in jumping animals *Perspectives in Experimental Biology* ed P Spencer Davies (Oxford: Pergamon)

Bennet-Clark H C 1977 Scale effects in jumping animals *Scale Effects in Animal Locomotion* ed T J Pedley (London: Academic)

Bennet-Clark H C and Lucey E C A 1967 The jump of the flea: a study of the energetics and a model of the mechanism *J. Exp. Biol.* **47** 59–76

Brackenbury J 1997 Caterpillar kinematics *Nature* **390** 453

Brackenbury J and Hunt H 1993 Jumping in springtails—mechanism and dynamics *J. Zool.* **229** 217–36

Brown B and Zeglin G 1998 The Bow Leg Hopping Robot *IEEE Int. Conf. on Robotics And Automation (Leuven, Belgium)*

Brown R H J 1967 Mechanism of locust jumping *Nature* **214** 939

Burrows M 2003 Froghopper insects leap to new heights *Nature* **424** 509

Caldwell R L 1979 A unique form of locomotion in a stomatopod—backward somersaulting *Nature* **282** 71–3

Davenport J 1994 How and why do flying fish fly *Rev. Fish Biol. Fisheries* **4** 184–214

Estier T, Crausaz Y, Merminod B, Lauria M, Piguet R and Siegwart R 2000 An innovative space rover with extended climbing alilities *Proc. Space and Robotics 2000 (Albuquerque, NM)*

Evans M E G 1973 The jump of the click beetle (Coleoptera : Elateridae)—energetics and mechanics *J. Zool.* **169** 181–94

Fiorini P and Burdick J 2003 The development of hopping capabilities for small robots *Auton. Robots* **14** 239–54

Full R, Earls K, Wong M and Caldwell R 1993 Locomotion like a wheel? *Nature* **365** 495

Gabriel J M 1984 The effect of animal design on jumping performance *J. Zool.* **204** 533–9

Garcia-Paris M and Deban S M 1995 A novel antipredator mechanism in Salamanders: rolling escape in hydromantes platycephalus *J. Herpetol.* **29** 149–51

Hale E, Schara N, Burdick J and Fiorini P 2000 A minimally actuated hopping rover for exploration of celestial bodies *Proc. 2000 IEEE Int. Conf. Robotics & Automation (San Fransisco, CA)*

Hayashi R and Tsujio S 2001 High-performance jumping movements by pendulum-type jumping machines *Proc. IEEE/RSJ—Int. Conf. Intelligent Robots And Systems (Maui, HI)*

Heitler W J 1974 Locust jump—specializations of metathoracic femoral-tibial joint *J. Comp. Physiol.* **89** 93–104

Henschel J R J 1990 Spiders wheel to escape *South African J. Sci.* **86** 151–2

Hill A V 1950 The dimensions of animals and their muscular dynamics *Sci. Prog.* **38** 209–30

Kaspari M and Weiser M D 1999 The size-grain hypothesis and interspecific scaling in ants *Func. Ecol.* **13** 530–8

Kikuchi F, Ota Y and Hirose S 2003 Basic performance experiments for jumping quadruped *Proc. 2003 IEEE/RSJ Int. Conf. Intelligent Robots And Systems (Las Vagas, NV)*
Liu J J 2005 Analysis of stairs-climbing ability for a tracked reconfigurable modular robot *Proc. 2005 IEEE Int. Workshop on Safety, Security and Rescue Robotics*
Morrey J M, Lambrecht B, Horchler A D, Ritzmann R E and Quinn R D 2003 Highly mobile and robust small quadruped robots *IEEE Int. Conf. Intelligent Robots and Systems*
Nakamura Y, Shimoda S and Shoji S 2000 Mobility of a microgravity rover using internal electro-magnetic levitation *Proc. 2000 IEEE/RJS Int. Conf. Intelligent Robots and Systems*
Okubo H, Nakano E and Handa M 1996 Design of a jumping machine using self-energizing spring *Proc. Iros 96. IEEE*
Paskins K E 2007 The mechanics and energy economy of animal jumping and landing applied to autonomous robots (Department of Mechanical Engineering, University of Bath)
Paskins K E, Bowyer A, Megill W M and Scheibe J S 2007 Takeoff and landing forces and the evolution of controlled gliding in northern flying squirrels (*Glaucomys Sabrinus*) *J. Exp. Biol.* **210** 1413–23
Paul C, Dravid R and Iida F 2002 Design and control of a pendulum driven hopping robot *IEEE/RSJ Int. Conf. Intelligent Robots and Systems (Lausanne, Switzerland)*
Quinn R D, Offi J T, Kingsley D A and Ritzmann R E 2002 Improved mobility through abstracted biological principles *IEEE/RSJ Int. Conf. Intelligent Robots and System (Lausanne, Switzerland)*
Raibert M H 1986 Legged robots *Commun. ACM* **29** 499–514
Rothschild M, Schlein J, Parker K, Neville C and Sternberg S 1975 The jumping mechanism of Xenopsylla cheopis *Phil. Trans. Roy. Soc.* B **271** 457–520
Shimoda S, Kubota T and Nakatani I 2002 New mobility system based on elastic energy under microgravity *Proc. Int. Symp. on Exp. Robotics (Washington, DC)*
Stoeter S A, Rybski P E, Gini M and Papanikolopoulos N 2002 Autonomous stair-hopping with scout robots *Proc. IEEE Int. Conf. Intelligent Robots And Systems (Lausanne, Switzerland)*
Sugiyama Y and Hirai S 2004 Crawling and jumping by a deformable robot *Proc. Int. Symp. on Experimental Robotics (Singapore)*
Vanezis A and Lees A 2005 A biomechanical analysis of good and poor performers of the vertical jump *Ergonomics* **48** 1594–603
Wei T, Nelson G M, Quinn R D, Verma H and Garverick S 2000 A 5 cm autonomous hopping robot *IEEE Conf. on Robotics and Automation (Icra '00) (San Francisco, CA)*
Weiss P 2001 Hop . . . Hop . . . Hopbots!: designers of small, mobile robots take cues from grasshoppers and frogs *Sci. News* **159** 88
Yoshimitsu T, Kubota T, Nakatani I, Adachi T and Saito H 2003 Micro-hopping robot for asteroid exploration *Acta Astronaut.* 441–6